RESEARCH ARTICLE

Macromolecular Materials and Engineering Open Access

www.mame-journal.de

Novel Linear Piezo-resistive Auxetic Meta-Sensors with Low Young's Modulus by a Core–Shell Conceptual Design and Electromechanical Modelling

Bahman Taherkhani, Mahdi Bodaghi,* Seyyed Sajad Mousavi Nejad Souq, Motaleb Malmir Chegini, and Mohammad Nemati*

Production of piezo-resistive auxetic sensors is usually carried out through mixing and coating methods. Although these methods are beneficial, Young's modulus of mixed sensors becomes high because of using a high percentage of sensing elements while the durability of coated sensors gets low due to the separation of sensing elements from the sensor surface. This article presents a new core–shell metamaterial model to address the mentioned problems. The shell and the core are produced of polydimethylsiloxane (PDMS) rubber and a mixture of PDMS/graphite powders (73.45 wt% graphite powders), respectively. A finite element model is developed via COMSOL software to predict the electromechanical behaviors of the created sensor and verified by an experimental study. Scanning electron microscope imaging is conducted to detect the separations of the graphite particles. The main important feature of this meta-sensor is to possess a linear sensitivity due to having zero Poisson's ratio. The advantage of this method is that Young's modulus of the sensor does not decrease (unlike the mixing method), and the sensor-coated particles do not separate from the sensor after a while (unlike the coating method). The introduced model has advantages that promote potential applications such as using sensory gloves to detect, for instance, human hand movements.

1. Introduction

The most important feature of auxetic structures is to have a negative Poisson's ratio (NPR).[1,2] They exhibit counter-intuitive deformation behaviors under uniaxial loading and become transversally thicker (thinner) under tension (compression).[3] Due to their extraordinary specifications, they have extensively been implemented in many fields including the medical industry,[4,5] actuation,[6] sports protection,[7] and sensors.[8] Auxetic materials have widely been used for manufacturing piezo-resistive sensors in recent years and provide extremely well sensing performance.[9,10] In fact, there have been numerous studies in recent years on sensor performance improvements achieved by methods based on sensor structure design. **Table 1** provides an overview of the research background on piezo-resistive sensors. According to Table 1, the main parameters affecting the sensing performance of the sensor are the substrate material[11–13] (e.g., two-components room temperature vulcanizing silicone (Silicone RTV2), polydimethylsiloxane (PDMS), Ecoflex, and thermoplastic polyurethane (TPU)), sensory element materials (e.g., graphene,[14–16] graphite,[17,18] carbon nanotubes (CNTs),[19–23] nanoparticles and nanowires[24]), manufacturing method (e.g., 3D printing,[25] mixing,[8,17,26,27] coating [14,28] and layer compositing[3,18]), and the structure of the sensor (e.g., conventional material, re-entrant auxetic structures,[8,18,29] constant Poisson's ratio (CPR) auxetic structures[17] and planar isotropic

B. Taherkhani
Faculty of Textile Technologies and Design
Textile Engineering Department
Istanbul Technical University
Istanbul 34437, Turkey
E-mail: taherkhani@itu.edu.tr

The ORCID identification number(s) for the author(s) of this article can be found under https://doi.org/10.1002/mame.202300219

DOI: 10.1002/mame.202300219

M. Bodaghi
Department of Engineering
School of Science and Technology
Nottingham Trent University
Nottingham NG11 8NS, UK
E-mail: mahdi.bodaghi@ntu.ac.uk

S. S. Mousavi Nejad Souq, M. Malmir Chegini
Department of Mechanical Engineering
Shahid Rajaee Teacher Training University
Tehran 1678815811, Iran

M. Nemati
Manufacturing and Production Group
A.S. Azimiyan Technical School
Qazvin 3416846435, Iran

Macromolecular Materials and Engineering Open Access
www.mame-journal.de

Table 1. The development of piezo-resistive sensors in terms of substrate material, sensing element, manufacturing method, and sensor structure.

Input parameters		Output parameters	
	two-components room temperature vulcanizing silicone (Silicone RTV2)		
Substrate material	Ecoflex		
	Polydimethylsiloxane (PDMS)		
	thermoplastic polyurethane (TPU)		
	carbon nanotubes (CNTs)		
Sensing element	Graphene		
	Graphite powders		Gauge factor
	Nano particles	**Electrical properties**	
	Coating		Sensitivity
Manufacturing method	3D printing		
	Mixing		
	Sandwich compositing		
	Conventional material		
Sensor structure	Re-entrant auxetic structure		
	Constant Poisson's ratio (CPR) auxetic structure		
	Isotropic auxetic structure with constant Poisson's ratio (CPR)		

auxetic structures [30]). The fourth case shows the connection between mechanical and electronic properties. The electronic properties can be engineered by changing the mechanical properties. The difference between the presented auxetic structures is an important parameter so-called variation of Poisson's ratio (ΔPR) during the strain. It causes a difference in the performance of the sensor. Output parameters include sensitivity and gauge factor.

To explain the importance of changing the structure and the importance of using the core–shell idea, a comparison between the re-entrant,[8] constant Poisson's ratio (CPR),[17] and planar isotropic[31] auxetic sensors with the same condition (including materials and manufacturing methods) showed that the sensory performance of the sensor will change by changing the structure. **Figure 1** shows the Poisson's ratio (PR) (a) and the sensitivity (b) in terms of the strain for the three mentioned sensors. The sensitivity curve is a function of the PR curve. Here, the lowest PR value for the re-entrant sensor corresponds to the highest sensitivity for this sensor. Because the PR is not constant, the sensitivity is also non-linear. The PR of the planar isotropic auxetic sensor has the highest value, which corresponds to the lowest sensitivity value, and due to the constant PR, the sensory performance is also linear. The CPR structure diagrams are between the other two sensor diagrams in both the PR and sensitivity. The idea of constructing a two-phase materials sensor for a re-entrant structure, the core–shell idea, was presented in our previous work.[3]

In this paper, the purpose of proposing the core–shell idea is that the sensors made by the coating method, although they have high sensing performance and low elastic modulus, they have low durability due to the separation of graphite particles. On the other hand, the sensors made by the mixing method

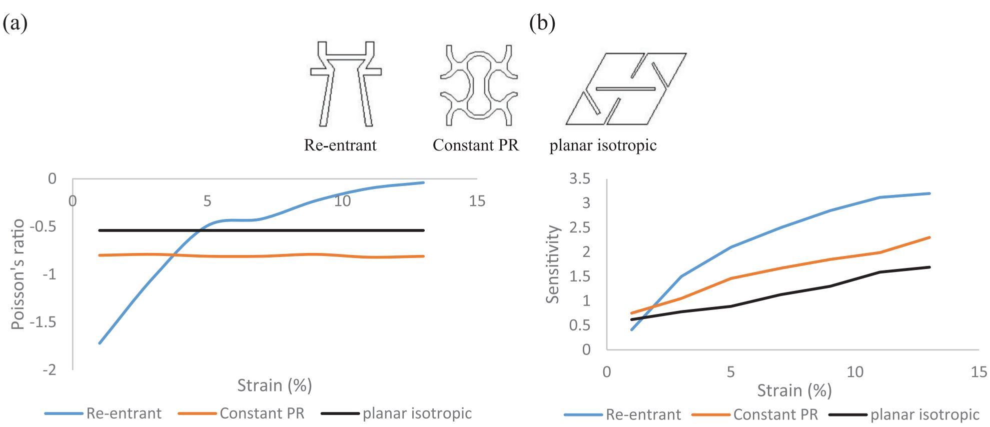

Figure 1. a) Poisson's ratio b) sensitivity of different auxetic structures used as piezo-resistive sensors.

provide long durability but have lower sensing performance and higher elastic modulus. In this article, an attempt has been made to establish a balance between sensory performance, elastic modulus, and the durability of the sensor by applying the core–shell idea. The use of the core–shell idea was presented in the literature review.[32] Hanwool Yeon et al.[32] implemented this idea to fabric perforated e-skins with inorganic physical sensors. Here, by applying the guidelines of this article,[32] a sensor with high durability, sensory performance, and elastic modulus between two mix and coating sensors is presented, and it showed that by putting two phases together, the sensory properties of the sensor can be better controlled. The graphite powder found in pencils was used as a sensory element, which is low-cost and available. For the base material, PDMS was used, which has a high flexibility. It is noteworthy that its flexibility will increase due to the addition of graphite powder (for the core material), which is compensated by applying the core–shell idea.

Previous works have investigated the possibility of controlling the sensory properties of piezo-resistive sensors by changing their structures.[33] The changes applied to the structure of metamaterials to convert a positive PR to a negative PR sometimes lead to the creation of a structure with zero Poisson's ratio (ZPR).[34–39] These structures have high energy absorption and have been the focus of many researchers in recent years. In this work, the main aim is to investigate the sensitivity of this group of metamaterials. It is worth nothing that the manufactured sensor has a linear sensing performance. Because the structure is unchanged in the transverse direction during the tension, and there will be longitudinal changes with a constant speed over time. Therefore, the sensory particles have a certain amount of space increase in each strain to create separation and create a linear sensory function. This article presents the piezo-resistive sensor, the strain is a variable, and the sensor performance test was performed in different strains.

In this work, a piezo-resistive sensor with a linear sensing performance was introduced through a metamaterial design with an approximate ZPR using core-sell idea. The substrate material, sensing element, and mold were selected as PDMS, graphite powders, and polylactic acid (PLA), respectively. A CNC machine was used to make the mold. Inside the mold, a series of protrusions were designed to create a series of grooves in the molded structure. These grooves were filled with a mixture of graphite powders (73.45% wt) and PDMS rubber to have a conductive sensor. The electromechanical behavior of the piezo-resistive sensors was simulated utilizing the COMSOL software package, and the results were verified with experimental data. The method that the sensor was made (core–shell idea) and the use of ZPR of the sensor during wide strain (linear sensor) made this sensor a suitable candidate for use in making sensory gloves to identify the movements of human fingers. The presented piezo-resistive sensor has a low Young's modulus due to its manufacturing method (core–shell idea). Here, the strain is a variable, and the sensing performance test was performed in different strains.

2. Experimental Section

The structure used in this work is the auxetic with a CPR, which was presented using the topology optimization method.[40] This work presented a piezo-resistive sensor from this structure using mixing[17] and coating[33] methods and compared their results. In this work, to create the ability to build a sensor with the core–shell idea, changes were made in this structure in such a way that the struts of the structure are thicker and the space is smaller so that the structure can be created in a two-phase manner. This change in geometry as well as the use of two materials in the structure resulted in a ZPR structure during the strain, which led to the creation of a sensor with linear sensing performance because there is no change in width in the transverse direction and the changes in the longitudinal direction are uniform and according to the description mentioned in our previous work,[33] the performance of the sensor will be linear. By combining the sensor input parameters, such as using the core–shell idea, the output parameters can be better controlled. Sensitivity and Gauge factor (GF) are calculated using Equations (1) and (2) as follows.

$$Sensitivity = \Delta R / R_0 \tag{1}$$

$$GF = \Delta R / R_0 . \varepsilon \tag{2}$$

in whichΔR, R_0 and ϵ are resistance difference, initial resistance and strain, respectively.

2.1. Material Property

The mechanical, electronic, and sensory properties of the sensor were examined separately to investigate its electromechanical behavior and to implement in the simulation part.

The auxetic[41–43] sensor materials include PDMS rubber and PDMS/graphite powder composite. The mechanical properties of each material were tested using a Zwick/Roell z100 universal testing machine. It has a 5 kN load cell, a displacement rate of 5 mm min^{-1}, and a capacity of 100 kN. For each material, using a mold made with a CNC milling machine, five dog bone samples were made according to the ASTM D412-06a standard, and each one was subjected to a tensile test. **Figure 2**a shows the dog bone die and molded dog bone for PDMS material (white specimen) and PDMS/graphite powder composite (black specimen). Figure 2b shows the tensile test setup. The results are presented in Figure 2c for PDMS material and Figure 2d for PDMS/graphite powder. Young's modulus for each material is estimated up to the range of elastic strain (5%) using the line.

To obtain the electronic properties, electrical conductivity and relative permittivity were determined. The Victor 86d digital multimeter, which can connect to a PC device, was implemented to obtain the mentioned parameters, and to record the electrical resistance changes. Simultaneously, the data is saved by implementing Hand DMM Data software. The sensor sensing performance test is done by producing a suitable fixture on a CNC milling machine. Figure 2e shows the shape of this fixture. To measure the sensor sensitivity, its resistance is measured and recorded at different moments. Figure 2f shows the experimental setup.

2.2. Sensor Preparation

The mold was designed and manufactured using Solidworks2014 software and the CNC milling machine coupled with the

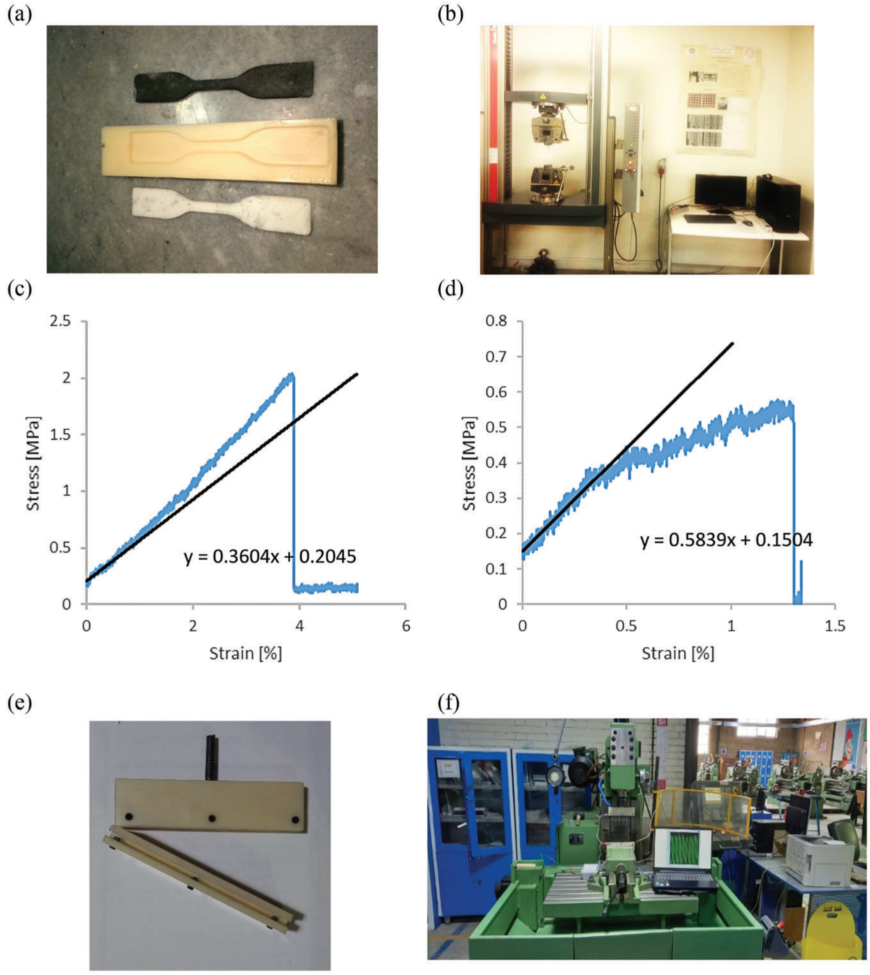

Figure 2. a) Dog bone die and doge bones for the constitutive materials of the core and shell b) tensile test setup. Mechanical property for c) Polydimethylsiloxane (PDMS) and (d) PDMS/graphite powder materials with the estimation of elastic modulus up to strain of 5%. e) The fixture to fix the sensor on the CNC milling device f) sensing performance test setup.

Edgecam2021 software, respectively in which the final sensor will be prepared as the core–shell idea with two different materials. To this end, the required details must be created in the mold considering the appropriate mold material selection. Therefore, the material of the mold is polylactic acid (PLA), which has high machinability, and it is possible to create details of the mold with high accuracy (first step of the sensor preparation). The importance of making the sensor as the core–shell model will be explained in detail in sec.4.

In the second step, the shell structure was molded using PDMS rubber and separates from the die after remaining in the open air for 2 h. PDMS is a two-part material and must mix with its hardener at a ratio of 10:1. In the third step, the core materials, a mixture of PDMS/ graphite powder (73.45 wt% of graphite powder) provided homogeneously using an electric mixer, are loaded on the structure. It was noted that for the core part, for PDMS to solidify, the hardener volume was calculated in terms of the PDMS amount, not the mixture of PDMS/graphite. For the core part, the percentage of graphite was 73.45% by weight compared to the PDMS material (regardless of the hardener). Then, the sensor was placed in the open air for 1 day and became one piece.

Figure 3 shows a schematic view of the sensor preparation. The SEM image was used to assess the distribution of graphite particles within the PDMS matrix. **Figure 4**a,b shows the front side and the back sides of the shell structure, respectively. As it is obvious from the figure, the front side of the shell is smooth, and the back side has channels for loading the core material. Figure 4c shows the details of the mold in the magnified view, and the presence of protrusions on it to create channels on the shell. Figure 4d displays the location of the core material on the shell.

3. Simulation Procedure

To study the sensitivity of the structure, in uniaxial loading, the geometry of the structure is created in the CAD design software, and then the sensitivity of the structure is extracted with the help of Solid Mechanical and Electrical Currents modules in the COMSOL software. The core–shell model of the structure is used according to the experimental work. The shell of the structure is made of PDMS (non-conductive), and the core of the structure is made of PDMS/ graphite powder particles (conductive). The simulations are performed as mechanical-electrical coupling and

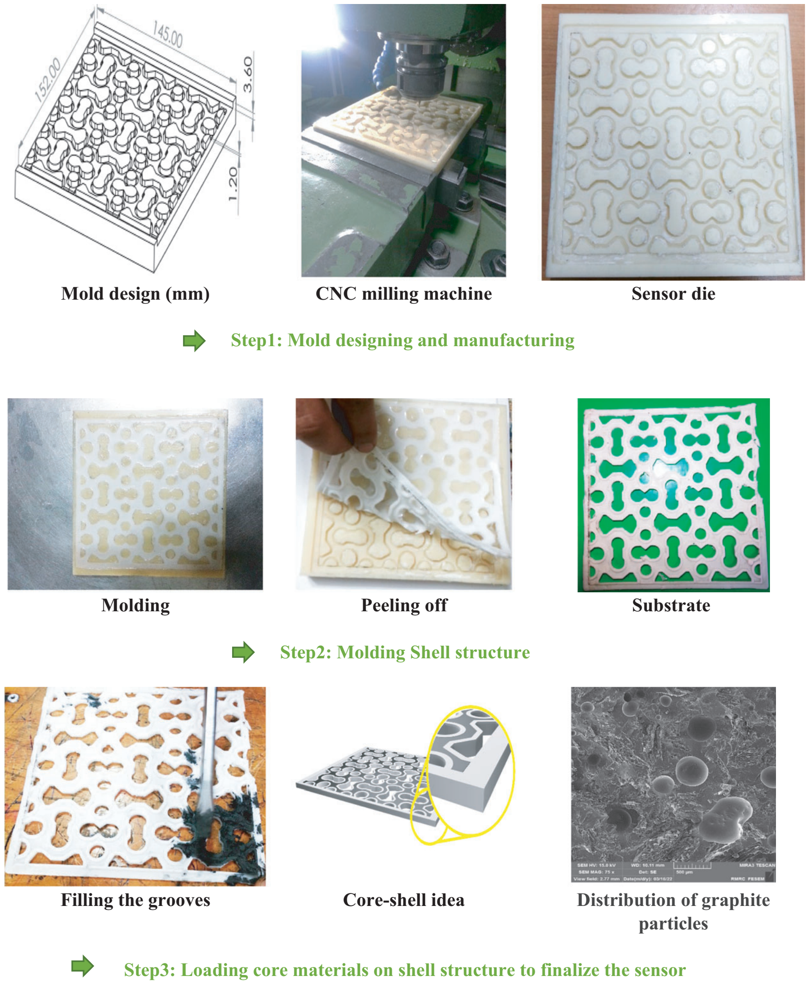

Figure 3. A schematic view of the sensor production.

time-dependent. The used modules have independent displacement variables (u, v, w) and electric potential variables (V) for the mechanical and electrical modules, respectively. The boundary condition chosen for the bottom boundary is to apply zero displacements (clamped) and zero potential (Ground). For the upper boundary, displacement (strain) is applied, and a current-type terminal with a value of 1A. During loading, the value of the voltage in the terminal compared to the initial voltage is considered as sensitivity (due to the constant current, the value of the voltage and electrical resistance are also the same). **Figure 5**a demonstrates the design of the core–shell model for the simulation of the presented sensor, and Figure 5b shows the boundary condition of the numerical study.

4. Results and Discussion

4.1. Deformation Behavior

In this work, the metamaterial with ZPR is investigated for using in the soft sensors field. Manufacturing a linear piezo-resistive auxetic sensor will be simple using constant ZPR metamaterial. The reason is that there is no change in width in the transverse direction, and the structure is increasing with a constant strain rate in the longitudinal direction. Therefore, the sensing elements in each strain have a certain amount of space increase to create separations, and as a result, the sensor performance will be linear.

In this part, the deformation of the structure, consisting of two materials with different mechanical properties, under tensile loading is evaluated. **Figure 6** illustrates the structure deformation during the strain experimentally and numerically. There is a good agreement between numerical and experimental results. During loading, from zero to about 10% strain, the sample remains planar. After this strain, the structure undergoes an out-of-plane displacement in the direction perpendicular to the plane which is consistent with the observation of experimental results. The reason is that it is made of two materials with different mechanical properties, and these materials cannot have the same deformation due to the application of the same displacement. It causes the structure deformation to take place out of the plane. **Figure 7** demonstrates the ZPR of the sensor during the strain (a) and out-of-plane deformation (b) numerically. **Figure 8**a shows the variation of the sensor PR and sensitivity during the strain experimentally and numerically.

Macromolecular Materials and Engineering Open Access
www.mame-journal.de

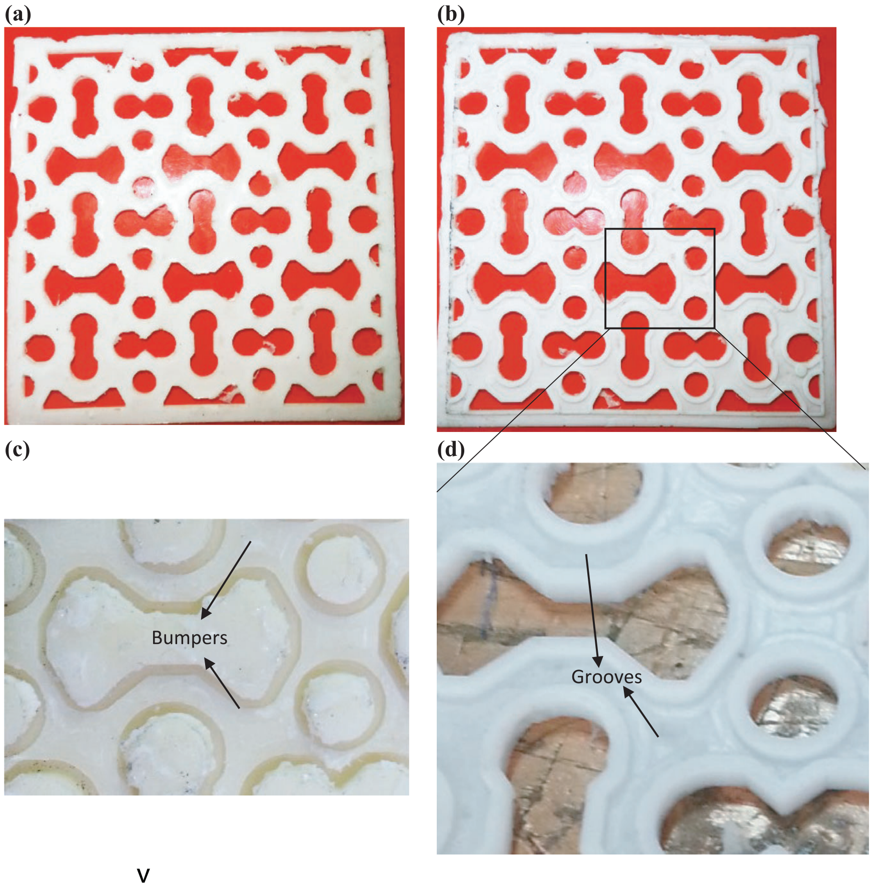

Figure 4. a) Front view and b) back view of the molded shell structure. c) Magnified view of the mold bump and d) the corresponded grooves in the molded structure.

4.2. Sensor Performance

The manufactured sensor has new ideas in terms of construction and selection of metamaterial structure. As Figure 8a shows, the sensing performance of the sensor is linear, which is caused by ZPR of the sensor structure during the strain of 24%. Therefore, one of the applications of metamaterials with ZPR is the use of these structures in the construction of linear piezo-resistive sensors. The use of linear sensors is important in making sensor gloves. Because there must be a one-to-one correspondence

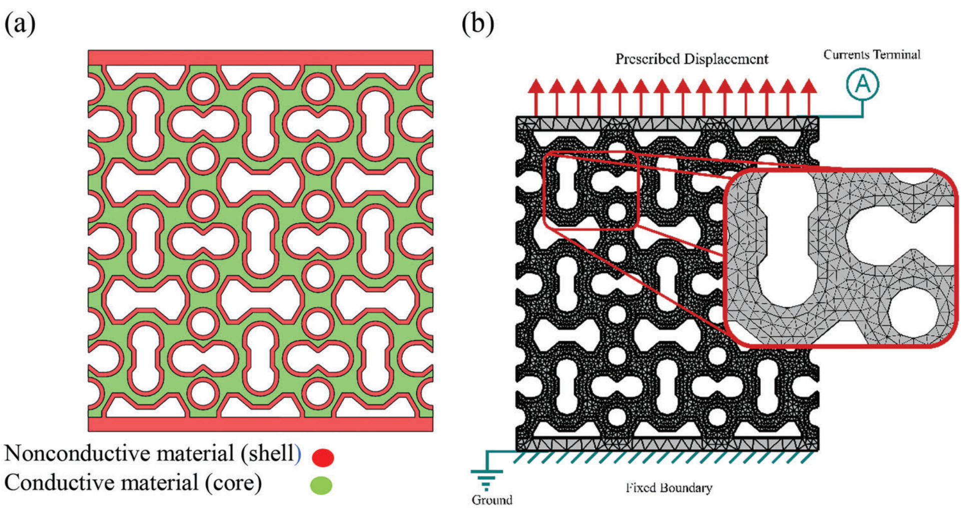

Figure 5. a) The simulation model of the sensor with two materials. b) Boundary conditions of the structure with ≈32 000 tetrahedral mesh.

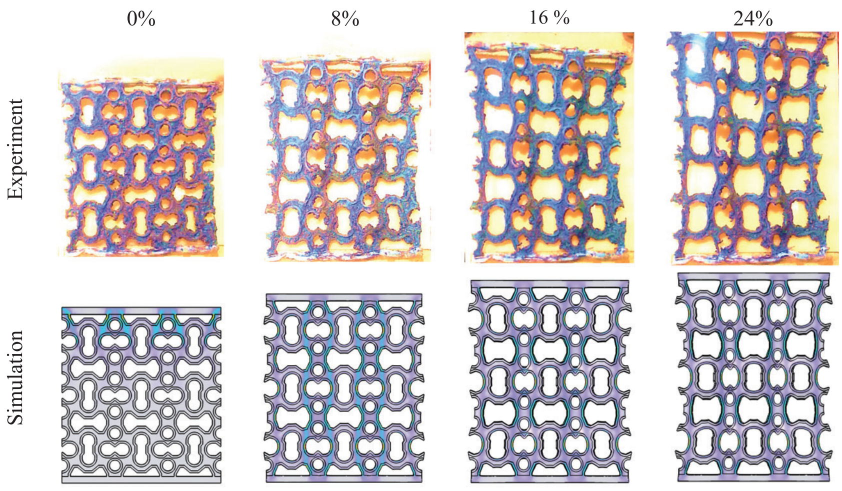

Figure 6. Deformation mechanism of the sensor during the strain experimentally and numerically.

between angle and resistance in order to detect finger movements in a one-to-one and linear way. Another advantage of this sensor is the use of the new core–shell idea in its construction. Because if coated sensors are used, the sensory particles of the sensor will be separated from the surface of the sensor after repeated use. If mixed sensors are used, the flexibility of the sensor is low and it cannot fit well on the fingers and detect finger movements well. Therefore, it is important to use the two ideas presented in this article to make a sensor in the application of sensor gloves.

The sensitivity test results of the sensor are presented for strains of 2% to 24% with an interval of 2% for each test. Figure 8b,c shows the sensor sensitivity in strains of 2%, and 24%, respectively. As can be seen, the proposed sensor has a linear sensing performance along the strain. To show the presented sensor cyclic durability, its sensing performance for 500 cycles of stretching/releasing is presented in Figure 8d.

Figure 9 and **Table 2** show the key parameters of the sensitivity between the presented sensor and conventional sandwich,[44] mixed CPR,[17] and coated CPR[33] sensors. The sensory performance of the conventional sandwich sensor is noticeably weaker than the auxetic sensors, which shows the importance of the auxeticity of the piezo-resistive sensors and has been repeatedly stated in the previous literature.[33] As can be seen, the proposed

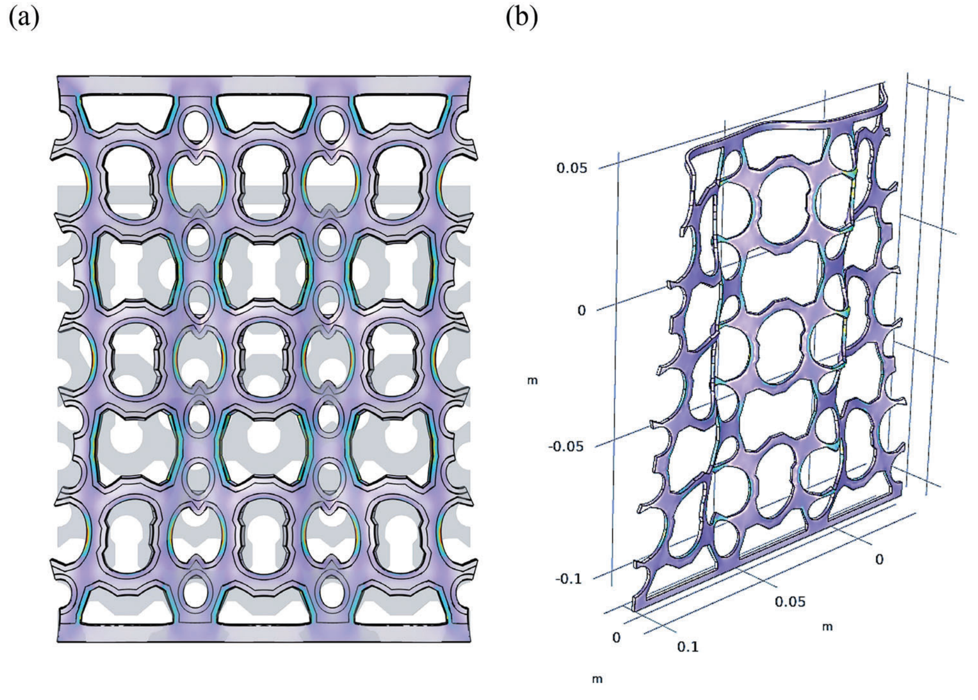

Figure 7. a) Exhibition of ZPR and b) out-of-plane deformation during the strain.

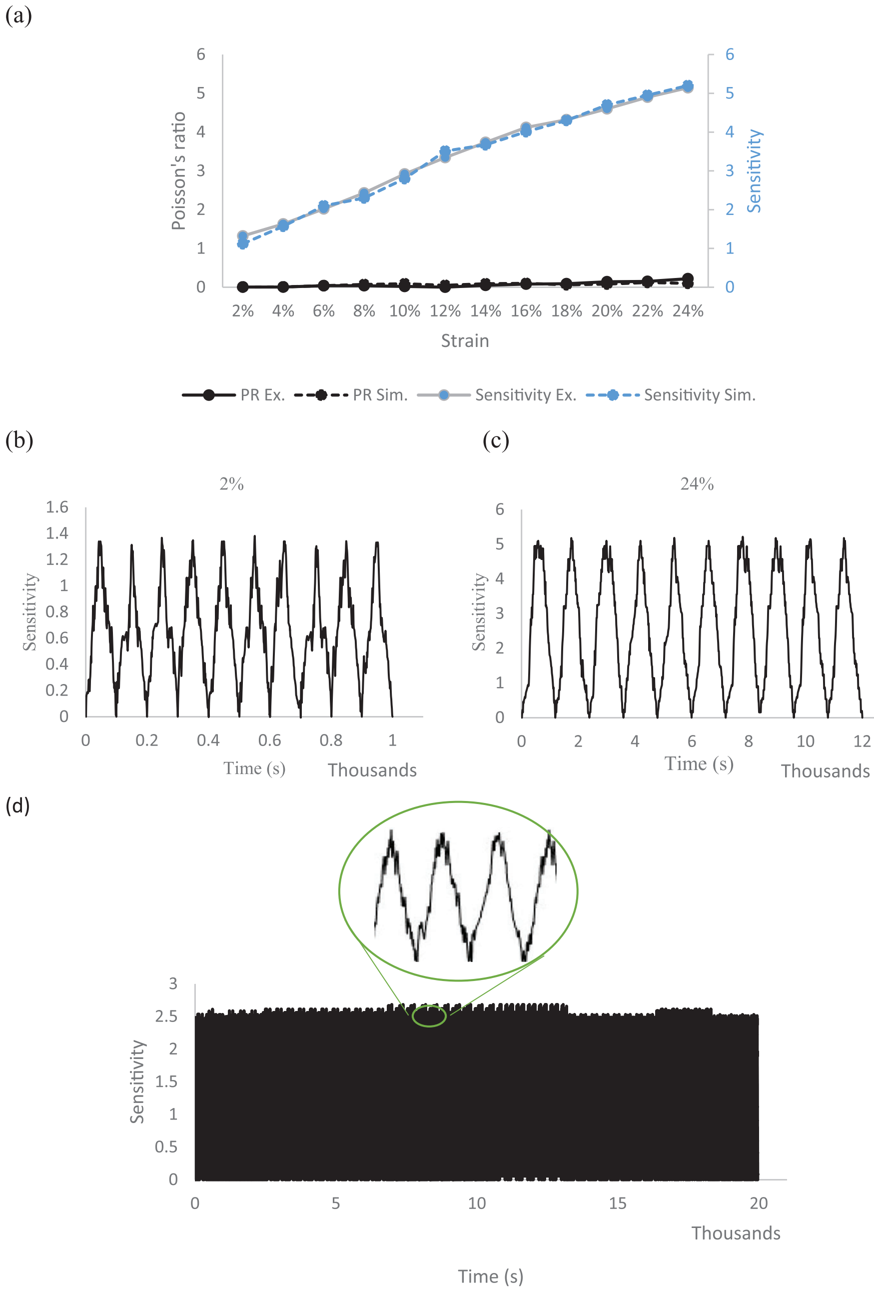

Figure 8. a) PR and sensitivity in terms of the strain for the proposed sensor experimentally and numerically. Sensing performance test for the strain of b) 2% and c) 24% and for d) 500 cyclic loading.

sensor has a weaker performance than the coated CPR sensor, but the noteworthy point is that it has high durability compared to mixed CPR sensors. The presented sensor has better sensory performance (35%) than the mixed CPR sensor, which is due to the use of the core–shell idea in its manufacturing process. In the next work, to apply this method, we want to use these sensors in making sensor gloves because they have high durability and better sensing performance in comparison with mixed CPR sensors. **Figure 10** shows scanning electron microscopy (SEM) images of the sensor before tensile loading (a) and after tensile loading (b).

5. Conclusion

In this work, a linear piezo-resistive metamaterial sensor with zero Poisson's ratio (ZPR) over a wide range of strains was presented. This sensor was innovative in terms of manufacturing technique and type of metamaterial structure used in the field of piezo-resistive sensors. The core–shell model technique was used in the sensor manufacturing process. The shell was made of polydimethylsiloxane (PDMS), which is highly flexible and non-conductive. The core was made of a mixture of PDMS and graphite (73.45% by weight of graphite powder) whose flexibility

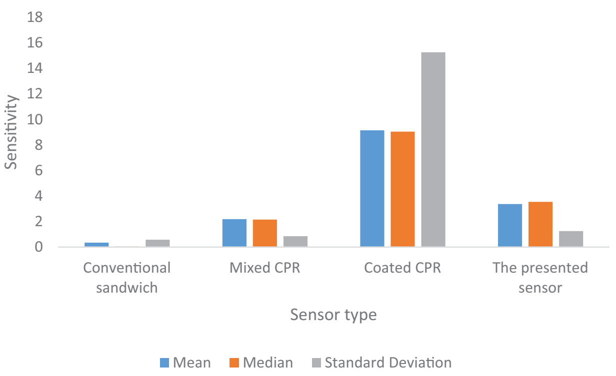

Figure 9. Comparison of the sensing performance of the previous researchers with the presented sensor in terms of mean, median, and standard deviation.

Table 2. Key parameters of the presented sensor and corresponding references.

Sensor type	Mean	Median	Standard deviation	Coefficient of variation	Variance
Conventional sandwich [44]	0.344	0.04	0.573	166.6	0.328
Mixed CPR [17]	2.19	2.15	0.849	38.77	0.721
Coated CPR [33]	9.15	9.05	15.27	166.89	233.17
The presented sensor	3.37	3.54	1.25	37.09	1.56

was reduced due to the presence of graphite, but it was conductive. The use of this technique provided and optimum state between durability and flexibility because the sensors made by the coated method have little durability, and the mixed sensors have little flexibility, but the provided sensor was simultaneously flexible and durable. The presented sensor had a better sensing performance of about 35% compared to the mix sensor made with a constant Poisson's ratio (CPR) auxetic structure with the same durability.

Another innovation of this work is the use of metamaterials with ZPR in a wide range of strains, which caused the sensor to have a linear sensing performance. Because this metamaterial structure did not change in dimensions in the transverse direction and increased in length in the longitudinal direction with a constant strain, the sensory elements in each strain had the same increase in space to create separations. In the next work, we will provide the glove sensor using the provided sensor in this work.

Acknowledgements

The authors would like to thank the 4D Materials and Printing Lab at Nottingham Trent University for providing software and hardware facilities for conducting this research. After initial online publication, Figures 2–9 and Table 2 were re-arranged on October 27, 2023, due to a previous error.

Conflict of Interest

The authors declare no conflict of interest.

Data Availability Statement

The data that support the findings of this study are available from the corresponding author upon reasonable request.

Keywords

auxetics, core–shell models, electro-mechanical simulation, low Young's modulus, metamaterials

Received: June 18, 2023
Revised: August 31, 2023
Published online:

[1] S. Rezaei, J. Kadkhodapour, R. Hamzehei, B. Taherkhani, A. P. Anaraki, S. Dariushi, *Photonics and Nanostruct. Fundam. Appl.* **2021**, *43*, 100868.
[2] B. Taherkhani, A. P. Anaraki, J. Kadkhodapour, S. Rezaei, H. Tu, *J. Elastomers Plast.* **2021**, *53*, 347.
[3] B. Taherkhani, *Fibers Polym.* **2023**, *24*, 1789,
[4] M. N. Ali, J. J. C. Busfield, I. U. Rehman, *J. Mater. Sci. Mater. Med.* **2014**, *25*, 527.

(a) (b)

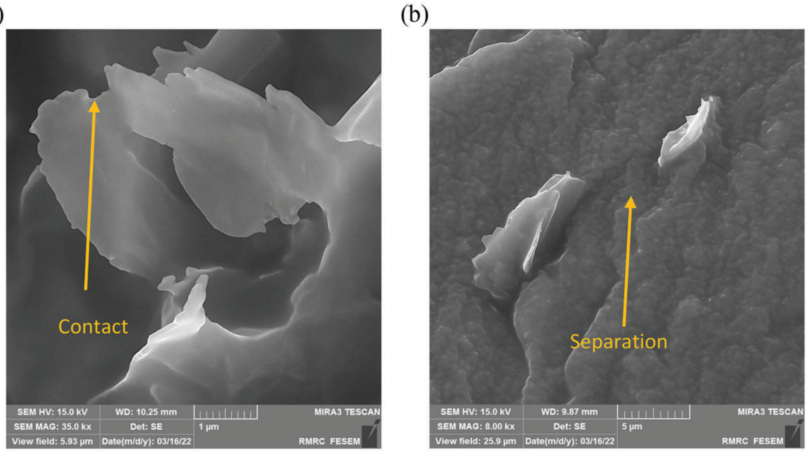

Figure 10. SEM images of the sensor (core) a) before the tensile loading and b) after tensile loading.

[5] K. Kuribayashi, K. Tsuchiya, Z. You, D. Tomus, M. Umemoto, T. Ito, M. Sasaki, *Mater. Sci. Eng., A.* **2006**, *419*, 131.
[6] J. I. Lipton, R. Maccurdy, Z. Manchester, L. Chin, D. Cellucci, D. Rus, *Science.* **2018**, *360*, 632.
[7] P. Giri, S. Kharkovsky, B. Samali, *Electronics.* **2017**, *6*, 36.
[8] B. Taherkhani, M. B. Azizkhani, J. Kadkhodapour, A. P. Anaraki, S. Rastgordani, *Sens. Actuators, A.* **2020**, *305*, 111939.
[9] P. U. Kelkar, H. S. Kim, K.-H. Cho, J. Y. Kwak, C.-Y. Kang, H.-C. Song, *Sensors.* **2020**, *20*, 3132.
[10] K. E. Evans, A. Alderson, *Auxetic Materials : Functional Materials and Structures from Lateral Thinking! Advanced Materials.* **2000**, *12*, 617.
[11] Y. Mao, W. Shen, S. Wu, X. Ge, F. Ao, Y. Ning, Y. Luo, Z. Liu, *React. Funct. Polym.* **2023**, *186*, 105568.
[12] N. V. Pol'shchikova, N. V. Sergienko, A. S. Belova, Y. N. Kononevich, D. S. Ionov, D. A. Khanin, M. I. Buzin, G. G. Nikiforova, O. I. Shchegolikhina, A. M. Muzafarov, *React. Funct. Polym.* **2023**, *186*, 105541.
[13] Y. Yoshino, M. Nakabayashi, S. Hayashi, *React. Funct. Polym.* **2023**, *186*, 105554.
[14] H.-B. Yao, J. Ge, C.-F. Wang, X. Wang, W. Hu, Z.-J. Zheng, Y. Ni, S.-H. Yu, *Adv. Mater.* **2013**, *25*, 6692.
[15] H. Tian, Y. Shu, Y.-L. Cui, W.-T. Mi, Y. Yang, D. Xie, T.-L. Ren, *Nanoscale.* **2014**, *6*, 699.
[16] J. Zhao, C. He, R. Yang, Z. Shi, M. Cheng, W. Yang, G. Xie, D. Wang, D. Shi, G. Zhang, *Appl. Phys. Lett.* **2012**, *101*, 063112.
[17] B. Taherkhani, M. M. Chegini, P. Rahmani, *Sens. Actuators, A.* **2022**, *345*, 113776.
[18] B. Taherkhani, J. Kadkhodapour, A. P. Anaraki, *Polym. Bull.* **2022**, *80*, 3745.
[19] S.-L. Gao, R.-C. Zhuang, J. Zhang, J.-W. Liu, E. Mäder, *Adv. Funct. Mater.* **2010**, *20*, 1885.
[20] J. Zhang, J. Liu, R. Zhuang, E. Mäder, G. Heinrich, S. Gao, *Adv. Mater.* **2011**, *23*, 3392.
[21] G. T. Pham, Y.-B. Park, Z. Liang, C. Zhang, B. Wang, *Composites, Part B.* **2008**, *39*, 209.
[22] D. J. Lipomi, M. Vosgueritchian, B. C.-K. Tee, S. L. Hellstrom, J. A. Lee, C. H. Fox, Z. Bao, *Nat. Nanotechnol.* **2011**, *6*, 788.
[23] T. Yamada, Y. Hayamizu, Y. Yamamoto, Y. Yomogida, A. Izadi-Najafabadi, D. N. Futaba, K. Hata, *Nat. Nanotechnol.* **2011**, *6*, 296.
[24] Y. Li, S. Luo, M.-C. Yang, R. Liang, C. Zeng, *Adv. Funct. Mater.* **2016**, *26*, 2900.
[25] T. Takahashi, K. Takei, A. G. Gillies, R. S. Fearing, A. Javey, *Nano Lett.* **2011**, *11*, 5408.
[26] S. Jung, J. H. Kim, J. Kim, S. Choi, J. Lee, I. Park, T. Hyeon, D.-H. Kim, *Adv. Mater.* **2014**, *26*, 4825.
[27] M. Wang, I. V. Anoshkin, A. G. Nasibulin, J. T. Korhonen, J. Seitsonen, J. Pere, E. I. Kauppinen, R. H. A. Ras, O. Ikkala, *Adv. Mater.* **2013**, *25*, 2428.
[28] E. Taer, W. S. Mustika, R. Taslim, *IOP Conference Series: Earth and Environmental Science.* **2017**, *58*, 012052.
[29] B. Taherkhani, A. Pourkamali Anaraki, J. Kadkhodapour, *J. Mech. Eng.* **2021**, *53*, 14.
[30] S. Shan, S. H. Kang, Z. Zhao, L. Fang, K. Bertoldi, *Extreme Mech Lett.* **2015**, *4*, 96.
[31] B. Taherkhani, S. Rahmani, O. Atalay, *Proc. Inst. Mech. Eng. Pt. L J. Mater. Des. Appl.* **2023**, https://doi.org/10.1177/14644207231174325.
[32] H. Yeon, H. Lee, Y. Kim, D. Lee, Y. Lee, J.-S. Lee, J. Shin, C. Choi, J.i-H. Kang, J. M. Suh, H. Kim, H. S. Kum, J. Lee, D. Kim, K. Ko, B. S. Ma, P. Lin, S. Han, S. Kim, S.-H. Bae, T.-S. Kim, M.-C. Park, Y.-C. Joo, E. Kim, J. Han, J. Kim, *Sci. Adv.* **2021**, *7*, eabg8459.
[33] B. Taherkhani, M. Bodaghi, S. Rahmani, F. Mesgari, *Adv. Eng. Mater.* **2003**, *25*, 2300524.
[34] Q. Qin, I. Dayyani, P. Webb, *Compos. Struct.* **2022**, *289*, 115455.
[35] Y. Chen, L. Ye, X. Han, *Compos. Struct.* **2022**, *293*, 115717.
[36] Q. Li, et al., A comparative study on mechanical and vibroacoustic performance of sandwich cylindrical shells with positive, negative, and zero Poisson's ratio cellular cores. Journal of Ocean Engineering and Science **2022**.
[37] Y. Chang, H. Wang, Q. Dong, *Mater. Today Commun.* **2022**, *30*, 103186.
[38] X. Chen, J. Moughames, Q. Ji, J. A. I. Martínez, H. Tan, S. Adrar, N. Laforge, J.-M. Cote, S. Euphrasie, G. Ulliac, M. Kadic, V. Laude, *Extreme Mech Lett.* **2020**, *41*, 101048.
[39] K. Liu, L. Han, W. Hu, L. Ji, S. Zhu, Z. Wan, X. Yang, Y. Wei, Z. Dai, Z. Zhao, Z. Li, P. Wang, R. Tao, *Mater. Des.* **2020**, *196*, 109153.
[40] A. Clausen, F. Wang, J. S. Jensen, O. Sigmund, J. A. Lewis, *Adv. Mater.* **2015**, *27*, 5523.
[41] L. Chow, K.-L. Yick, K. H. Wong, M. S.-H. Leung, Y. Sun, M.-Y. Kwan, K. Ning, A. Yu, J. Yip, Y.-F. Chan, S.-P. Ng, *Macromol. Mater. Eng.* **2022**, *307*, 2100866.
[42] G. Flamourakis, I. Spanos, Z. Vangelatos, P. Manganas, L. Papadimitriou, C. Grigoropoulos, A. Ranella, M. Farsari, *Macromol. Mater. Eng.* **2020**, *305*, 2000238.
[43] Z. Guo, X. Peng, L. Sang, *Macromol. Mater. Eng.* **2020**, *305*, 2000355.
[44] M. Azizkhani, S. Rastgordani, A. P. Anaraki, J. Kadkhodapour, B. S. Hadavand, *J. Compos. Mater.* **2020**, *54*, 423.